

---

# CDLM: CONSISTENCY DIFFUSION LANGUAGE MODELS FOR FASTER SAMPLING

---

Minseo Kim<sup>1</sup> Chenfeng Xu<sup>2,3</sup> Coleman Hooper<sup>2</sup> Harman Singh<sup>2</sup> Ben Athiwaratkun<sup>3</sup> Ce Zhang<sup>3</sup>  
Kurt Keutzer<sup>2</sup> Amir Gholami<sup>2</sup>

## ABSTRACT

Diffusion Language Models (DLMs) offer a promising parallel generation paradigm but suffer from slow inference due to numerous refinement steps and the inability to use standard KV caching. We introduce CDLM (Consistency Diffusion Language Models), a training-based acceleration method that simultaneously tackles both bottlenecks. CDLM integrates consistency modeling to drastically reduce the number of required sampling steps by enabling multi-token finalization. Furthermore, we enforce a block-wise causal attention mask during fine-tuning, making the model fully compatible with KV caching. Experiments show CDLM achieves  $3.6\times$ – $14.5\times$  lower latency while maintaining competitive accuracy on math and coding tasks. The full training and evaluation code is available at <https://github.com/SqueezeAILab/CDLM>.

## 1 INTRODUCTION

Large Language Models (LLMs) have triggered a paradigm shift in AI, excelling at tasks such as instruction following, multi-turn dialogue, and code generation (OpenAI, 2023). Most current LLMs are autoregressive, decoder-only Transformers trained to predict the next token under a causal attention mask (Dubey et al., 2024; Zhang et al., 2022). While training is parallelizable via teacher forcing, inference inherits a rigid sequential dependency, becoming a key efficiency bottleneck. Moreover, such models cannot exploit bidirectional context, which limits performance on tasks such as text infilling, editing, and global planning (Hu et al., 2024; Song et al., 2025).

As a promising alternative, diffusion language models (DLMs) have drawn attention for their potential in text generation. Inspired by the success of diffusion models in image, audio, and video synthesis (Ho et al., 2020), DLMs iteratively denoise random or masked token sequences into coherent text (Gong et al., 2023; Li et al., 2022). This process updates all token positions *in parallel* per step, removing the token-level sequential dependency inherent to autoregressive decoding. Closed-source models, primarily in code generation, report up to  $10\times$  higher throughput than autoregressive models while preserving quality (Google DeepMind, 2025; Khanna et al., 2025; Song et al., 2025). How-

ever, open-source DLMs remain significantly slower (Nie et al., 2025b; Ye et al., 2025), largely because (1) bidirectional attention prohibits standard KV caching and (2) they demand many refinement steps, often proportional to sequence length, to reach high fidelity (Kim et al., 2025).

Many recent works aim to accelerate DLM inference. One primary strategy leverages block-wise decoding with KV caching, either via approximate caching with periodic updates (Hu et al., 2025; Liu et al., 2025; Ma et al., 2025; Wu et al., 2025b) or by fine-tuning the model into a fully block-wise causal architecture so that caching becomes natural (Wang et al., 2025; Wu et al., 2025a). The other major line of work focuses on parallel sampling algorithms, which effectively decode multiple tokens per denoising step and reduce the total number of iterations (Ben-Hamu et al., 2025; Wu et al., 2025b).

Turning to diffusion-based applications in vision domains, many works have successfully reduced denoising to few-step or even one-step generation (Yin et al., 2024; 2025). A prominent technique in that realm is *consistency modeling*: consistency models are trained to minimize discrepancies between adjacent denoising states along the probability flow ODE, enabling near one-step generation (Song et al., 2023; Song & Dhariwal, 2023). Although originally developed for continuous data, the consistency paradigm has begun to influence discrete settings, including parallel decoding for autoregressive language models (Kou et al., 2024) and masked diffusion frameworks (Xu et al., 2025b), indicating its strong promise in discrete language domains.

To drive DLMs to converge to coherent text in far fewer

---

<sup>1</sup>Seoul National University, Seoul, South Korea <sup>2</sup>University of California, Berkeley, CA, USA <sup>3</sup>Together AI, San Francisco, CA, USA. Correspondence to: Amir Gholami <amirgh@berkeley.edu>.

refinement steps, we present **CDLM**, a training-based acceleration method that integrates Consistency modeling into **Diffusion Language Models**. Concretely, the student is trained to finalize multiple tokens per step by distilling from a fully bidirectional teacher and by aligning its predictions between a less-informed state and its block-completion state along the decoding trajectory. We impose a block-wise causal attention mask and jointly optimize three objectives. At inference time, the model decodes sequentially over blocks while applying confidence-thresholded parallel decoding within each block. This design directly tackles two core bottlenecks of current DLMs: (i) excessive sampling steps (mitigated by distillation and consistency) and (ii) cache inefficiency (removed by block-wise causality). In particular, we make the following contributions:

- **Consistency-guided distillation.** We bring consistency modeling to DLMs by defining a token-level decoding trajectory and coupling it with distillation from a fully bidirectional teacher. This joint objective provides explicit supervision for multi-token finalization while keeping predictions stable within each block (see Sections 3 and 4.2).
- **Cache-friendly block causality.** By fine-tuning with a block-wise causal attention mask (Figure 2), we enable bidirectional DLMs to support block-wise KV caching and early stopping at block boundaries (see Sections 4.1 and 4.3).
- **End-to-end speedups.** With 8 hours of training for Dream and 16 hours for LLaDA, CDLM cuts refinement steps by  $3.4\times$ – $7.9\times$  and latency by  $3.6\times$ – $14.5\times$  while maintaining accuracy across math and coding benchmarks. It also surpasses equal-size autoregressive LLMs in tokens-per-second (see Section 5.2).

## 2 BACKGROUND

Here, we briefly review relevant background.

### 2.1 Diffusion Language Models

Diffusion models (Ho et al., 2020) have been successfully applied across modalities such as text-conditioned image generation (Ramesh et al., 2022), audio synthesis (Chen et al., 2021b), and video generation (Esser et al., 2023). In language modeling, diffusion language models (DLMs) generate fixed-length sequences via iterative refinement: at each step, multiple token positions are updated in parallel and finalized (Gong et al., 2023; Li et al., 2022). Early approaches operated in the continuous embedding space (Gao et al., 2024b; Gong et al., 2023), but more recent models adopt masked diffusion models (MDMs) that work directly in the discrete token space (Gong et al., 2025a; Nie et al., 2025a).

They begin from a fully masked sequence and iteratively unmask tokens according to a scheduling policy. In this paper, we treat MDMs as the representative class of DLMs, especially Dream (Ye et al., 2025) and LLaDA (Nie et al., 2025b). Architecturally, DLMs commonly employ Transformer backbones with *bidirectional* (non-causal) attention, permitting full-context interactions (Nie et al., 2025b). Despite their parallel update capability, DLMs are known to be slow for two main reasons. First, full bidirectional attention at every step renders them incompatible with standard KV caching. Second, high-quality generation typically demands a large number of refinement steps comparable to the sequence length, making inference inefficient (Kim et al., 2025). In this work, we propose a fine-tuning-based solution that addresses both limitations.

### 2.2 Efficient Inference in Diffusion Language Models

Inference in DLMs is an active area of research with significant room for improvement. Among training-free acceleration methods, one line of work exploits approximate caching via block-wise decoding, refreshing static regions periodically (Ma et al., 2025; Wu et al., 2025b). Others speed up parallel sampling by applying confidence thresholds (Wu et al., 2025b) or by leveraging lightweight autoregressive models as guidance (Hu et al., 2025). In contrast, training-based approaches focus on improving the intrinsic efficiency of DLMs through architectural or objective-level modifications. Some recent works fine-tune models to introduce block-wise causality, enabling standard KV caching at the block level while retaining diffusion-style updates within each block (Wang et al., 2025; Wu et al., 2025a). Others design objectives that promote faster convergence by encouraging high-confidence token prediction (Chen et al., 2025). Our method is training-based: we induce block-wise causality and cut refinement steps via fine-tuning.

### 2.3 Knowledge Distillation in Language Models

Knowledge distillation (KD) (Hinton et al., 2015) transfers knowledge from a large, powerful teacher to a smaller, more efficient student. In early LLM work, KD was largely *black-box*, where students imitated textual outputs from closed-source APIs (Fu et al., 2023). With the rise of open-source LLMs, *white-box* distillation became feasible, enabling direct supervision from the teacher’s internal representations, such as logits or embeddings (Agarwal et al., 2024; Gu et al., 2023). Beyond language modeling, distillation has also been successfully applied to diffusion-based image and video generation to cut sampling steps while preserving quality (Yin et al., 2024; 2025). Our method can similarly be viewed as a form of *self-distillation*: we distill knowledge from a teacher to a student of identical size and model type, but with different architectural design (a fully bidirectional teacher vs. a block-wise causal student). We adopt a white-box setup

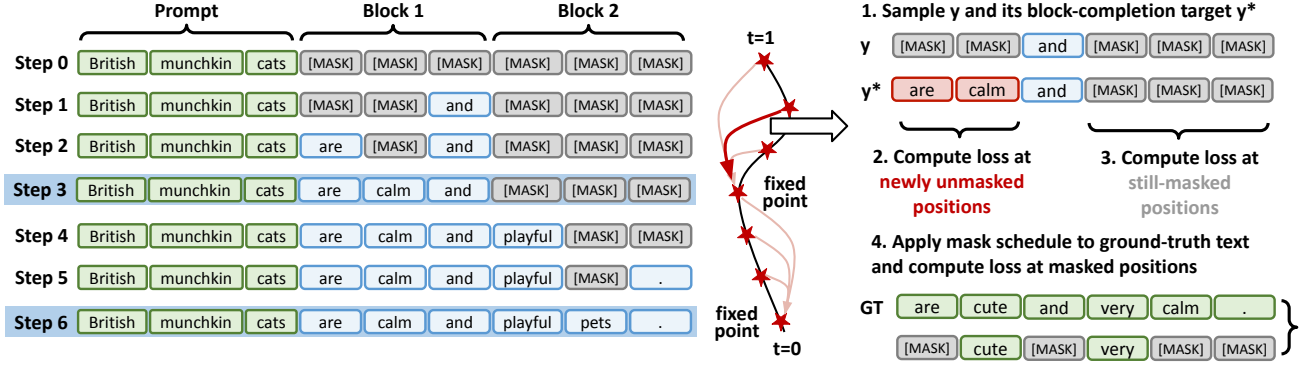


Figure 1. **Left:** Block-wise decoding trajectory of the teacher (steps  $0 \rightarrow N$ ; diffusion time  $t : 1 \rightarrow 0$ ). **Right:** The student’s three-objective loss at an intermediate state  $y$ : (i) distillation from teacher logits on newly unmasked positions, (ii) consistency between  $y$  and its block-completion  $y^*$ , and (iii) masked-denoising (DLM) loss on randomly masked ground-truth text.

with rich intermediate supervision, enabling efficient and stable knowledge transfer. Like Deschenaux & Gulcehre (2025) and Xu et al. (2025a), we reduce decoding steps by distilling multi-step diffusion trajectories into *jumps* between non-consecutive denoising states. Our novelty is to instantiate these jumps in a block-causal student, and to train it with *consistency*-oriented objectives.

## 2.4 Consistency Models and Language Models

Consistency models (Song et al., 2023) were introduced to overcome the slow, iterative sampling process of diffusion models. They learn a *consistency* property: any intermediate state along a probability flow ODE trajectory can be mapped directly back to its origin (the clean data), enabling near one-step generation. (Song & Dhariwal, 2023). While originally developed for continuous domains such as vision, recent work has explored adapting this idea to discrete language modeling (Kou et al., 2024; Xu et al., 2025b). Rather than explicitly modeling the ODE solver or its continuous trajectory, these methods reinterpret the notion of mapping intermediate states to final solutions within discrete token trajectories. For instance, autoregressive language models, despite lacking an explicit diffusion trajectory, realize this principle via Jacobi-style parallel decoding, treating iterative drafts as intermediate states (Santilli et al., 2023). Our approach adopts this paradigm in DLMs, where trajectories arise naturally from iterative denoising. Conceptually, our objective can be viewed as an empirical generalization of the original consistency objective defined over continuous ODE trajectories, adapted to discrete, token-level diffusion processes.

## 3 PRELIMINARY: INFERENCE IN DIFFUSION LANGUAGE MODELS

We formalize DLM inference by defining the iterative refinement process, the sampling strategies, and the decoding

trajectory that underpins our training objectives.

**Iterative Refinement Process.** DLM generation is an iterative refinement over  $N$  discrete sampling steps. It gradually transforms a fully masked sequence  $\mathbf{x}_1$  at time  $t = 1$  (step 0) into a clean sequence  $\mathbf{x}_0$  at  $t = 0$  (step  $N$ ). Here,  $N$  serves as a hyperparameter controlling the trade-off between generation speed and sample quality. We denote the sequence at a discrete step  $k$  (where  $k = 0, 1, \dots, N$ ) as  $\mathbf{x}_{t_k}$  with  $t_k = 1 - \frac{k}{N}$  (so  $t_0=1, t_N=0$ ). At each step, approximately  $L_g/N$  tokens are finalized on average, where  $L_g$  is the target generation length.

This refinement process is modeled probabilistically. Specifically, the transition from a state  $\mathbf{x}_t$  to a subsequent state  $\mathbf{x}_s$   $0 \leq s < t \leq 1$  is governed by the model  $p_\theta$ ’s prediction of the clean sequence  $\mathbf{x}_0$  given the current noisy sequence  $\mathbf{x}_t$  and a conditioning prompt  $c$ , i.e.,

$$p_\theta(\mathbf{x}_0 \mid \mathbf{x}_t, c). \quad (1)$$

Following prior formulations (Austin et al., 2021a), the reverse-time transition  $q_{s|t}(\mathbf{x}_s \mid \mathbf{x}_t)$  is defined for  $0 \leq s < t \leq 1$  and factorizes across tokens. For each token  $i$ , the transition probability is defined as:

$$q_{s|t}(x_s^i \mid x_t^i) = \begin{cases} 1, & \text{if } x_t^i \neq [\text{MASK}], x_s^i = x_t^i, \\ \frac{s}{t}, & \text{if } x_t^i = [\text{MASK}], x_s^i = [\text{MASK}], \\ \frac{t-s}{t} q_{0|t}(x_s^i \mid \mathbf{x}_t, c), & \text{if } x_t^i = [\text{MASK}], x_s^i \neq [\text{MASK}]. \end{cases} \quad (2)$$

where  $q_{0|t}$  is the predictive distribution induced by  $p_\theta(\mathbf{x}_0 \mid \mathbf{x}_t, c)$ . This formulation captures three possibilities: (1) an already-unmasked token remains unchanged, (2) a masked

token remains masked, or (3) a masked token is unmasked to a new token.

**Sampling Strategies.** To instantiate the probabilistic distribution  $q_{s|t}$  into an actual generation procedure, practical deterministic strategies are employed. A common choice is *low-confidence remasking*, where instead of stochastic sampling, the model greedily selects the tokens to unmask (Nie et al., 2025b). Based on the confidence scores from  $p_\theta(\mathbf{x}_0 | \mathbf{x}_t, c)$ , the top- $m$  masked tokens with the highest probabilities are revealed, while all others remain masked. In practice, this process is often constrained to operate within *blocks* of tokens, called *block-wise decoding*, limiting unmasking to localized regions of the sequence. This prevents unnatural early generation (e.g., premature `<endoftext>` tokens) (Nie et al., 2025b) and, more importantly, enables KV caching for finalized blocks.

**Decoding Trajectory.** Given this iterative and probabilistic refinement process, we define the *decoding trajectory*  $\mathcal{T}$  as the sequence of states that the model traverses during inference:

$$\mathcal{T}_x = (\mathbf{x}_{t_0}, \mathbf{x}_{t_1}, \dots, \mathbf{x}_{t_N}), \quad t_k = 1 - \frac{k}{N}. \quad (3)$$

Each  $\mathbf{x}_{t_k}$  is a partially refined sequence; the trajectory  $\mathcal{T}_x$  records its evolution across steps. Figure 1 (left) visualizes an example. This trajectory serves as the foundation for our consistency-based training below.

## 4 METHODOLOGY

We present **Consistency Diffusion Language Models (CDLM)**, a training scheme that accelerates DLM inference without sacrificing quality. We first describe how we collect teacher decoding trajectories and store compact hidden states for logit reconstruction, then introduce the distillation, consistency, and DLM objectives, and finally detail our confidence-thresholded block-wise inference.

### 4.1 Trajectory Collection for Diffusion Language Models

**Data Generation** Let  $p_\theta$  denote the teacher DLM and  $q_\phi(\cdot | x)$  the student DLM initialized from the teacher’s weights. The teacher uses a *bidirectional* attention mask as in standard DLMs, whereas the student is trained with a *block-wise causal* mask, as illustrated in Figure 2. To enable consistency training, we collect trajectories offline by running the teacher on domain-specific prompts. For each prompt  $x$ , we denote the token-level trajectory as  $\mathcal{T}_x$  and the corresponding hidden-state buffer by  $\mathbf{H}_x \in \mathbb{R}^{L_g \times d}$ ; the resulting dataset is  $\mathcal{D} = \{(x, \hat{y}, \mathcal{T}_x, \mathbf{H}_x)\}$  with ground-truth text  $\hat{y}$  included. The overall procedure is summarized

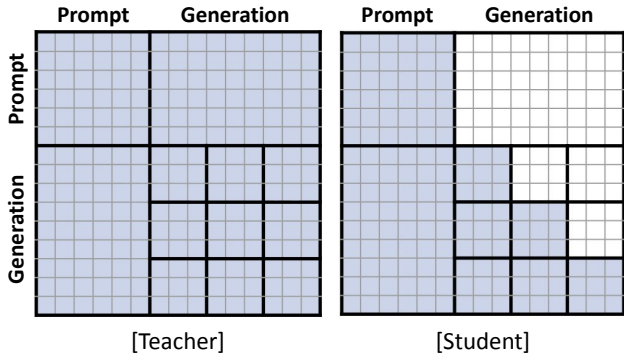


Figure 2. **Left:** Teacher DLM with full bidirectional attention, attending to the entire context. **Right:** Student DLM with a block-wise causal mask, attending to the prompt, previously completed blocks, and the current decoding block.

in Algorithm 1.

Prior work reports that block-wise decoding is effective for instruction-tuned models and attains high quality when the number of steps matches the generation length (Nie et al., 2025b). Accordingly, we adopt block-wise decoding with the number of sampling steps equal to the generation length ( $N=L_g$ ) and finalize exactly one token per step within the current block (the highest-confidence token  $y_i$ ). This configuration places the teacher at its most performant operating point and yields higher-quality trajectories. For white-box distillation, we store not only  $\mathcal{T}_x$  but also the states required to reconstruct logits. Concretely, we record the last hidden states at the moments when tokens are finalized.

**Data Augmentation** Effective training benefits from trajectories that are both diverse and reliable. Unlike autoregressive models, where temperature only influences token selection, in DLMs, the temperature also changes the order in which tokens are revealed (Gong et al., 2025b) which allows further diversity in the generated data. We therefore augment each prompt with multiple trajectories generated at different temperatures. Additional details on dataset construction are provided in Appendix A.1.

### 4.2 Training

We jointly minimize three objectives to train CDLMs: (i) a **Distillation loss** that transfers the teacher’s multi-token finalization signal to the block-wise causal student; (ii) a **Consistency loss** that enforces within-block temporal consistency between two states; and (iii) a **DLM loss** that preserves the model’s masked-token prediction capability. The detailed training procedure is depicted in Algorithm 2.

**Notation** Given the dataset  $\mathcal{D} = \{(x, \hat{y}, \mathcal{T}_x, \mathbf{H}_x)\}$ , we first sample a prompt  $x$  and its trajectory  $\mathcal{T}_x$ , then sample a state  $y \in \mathcal{T}_x$  and its block-completion state  $y^*$ . Here,  $y^*$

**Algorithm 1** Trajectory Collection for Training CDLM

- 1: **Input:** dataset  $\mathcal{O}$  of pairs  $(x, \hat{y})$ , generation length  $L_g$ , block size  $B$ , total steps  $N=L_g$ , teacher DLM  $p_\theta$ , temperature set  $\mathcal{S}_\tau$ , target count  $n$
- 2: **Output:** dataset  $\mathcal{D}$  of quadruples  $(x, \hat{y}, \mathcal{T}_x, \mathbf{H}_x)$
- 3: Initialize  $\mathcal{D} \leftarrow \emptyset$
- 4: **repeat**
- 5:   Sample  $(x, \hat{y}) \sim \mathcal{O}$ ; build input ids  $\mathbf{x}$  with the answer span masked
- 6:   **for** each temperature  $\tau \in \mathcal{S}_\tau$  **do**
- 7:      $\mathcal{T} \leftarrow []$ ;  $\mathbf{H} \leftarrow \mathbf{0} \in \mathbb{R}^{L_g \times d}$
- 8:     **for** blocks  $b = 1, \dots, \lceil L_g/B \rceil$  **do**
- 9:       **for** steps  $s = 1, \dots, B$  **do**
- 10:          Run  $p_\theta(\mathbf{x})$ ; obtain logits  $\ell$  and last hidden  $\mathbf{h}$
- 11:          Sample  $\mathbf{y}$  and compute confidence  $\mathbf{c}$
- 12:          Finalize top-1 token  $y_i$  in the current block; write  $\mathbf{h}_i \rightarrow \mathbf{H}$ ; append  $\mathbf{x} \rightarrow \mathcal{T}$
- 13:       **end for**
- 14:     **end for**
- 15:     Append  $(x, \hat{y}, \mathcal{T}, \mathbf{H})$  to  $\mathcal{D}$
- 16:   **end for**
- 17: **until**  $|\text{processed\_pairs}| \geq n$

denotes the state obtained by fully unmasking the active block of  $y$  (thus  $y$  and  $y^*$  are at most  $B$  steps apart). The right panel of Figure 1 visualizes this setup. We denote  $\mathcal{U}_y = \{i \mid y_i = [\text{MASK}], y_i^* \neq [\text{MASK}]\}$  as the newly unmasked token indices between  $y$  and  $y^*$ , and  $\mathcal{S}_y = \{i \mid y_i = [\text{MASK}], y_i^* = [\text{MASK}]\}$  as the still-masked token indices at  $y^*$ .

**Distillation Loss** We use the student’s predictions at state  $y$  together with the teacher’s hidden-state buffer  $\mathbf{H}_x$ . For each  $i \in \mathcal{U}_y$ , we reconstruct the teacher’s distribution by applying  $\ell_i^{(T)} = \text{lm\_head}(\mathbf{h}_{x,i})$  and  $p_i^{(T)} = \text{softmax}(\ell_i^{(T)})$  to the stored hidden state  $\mathbf{h}_{x,i}$ . With these teacher distributions, we define the distillation objective as

$$\mathcal{L}_{\text{Distillation}} = \mathbb{E}_{(x, \mathcal{T}_x, \mathbf{H}_x) \sim \mathcal{D}} \mathbb{E}_{y \sim \mathcal{T}_x} \left[ \frac{1}{|\mathcal{U}_y|} \sum_{i \in \mathcal{U}_y} D_{\text{KL}}(p_i^{(T)} \parallel q_\phi(\cdot \mid y, x)_i) \right], \quad (4)$$

which applies forward KL divergence on the positions newly unmasked between  $y$  and  $y^*$ . This serves as the main anchor that transfers the bidirectional teacher’s guidance to the block-wise student, effectively providing *supervision for multi-token finalization* within each block.

**Consistency Loss** We compare the student’s predictive distributions at state  $y$  and block-completion state  $y^*$ , enforcing agreement on still-masked positions. Concretely,

**Algorithm 2** Training Algorithm for CDLM

- 1: **Input:** dataset  $\mathcal{D} = \{(x, \hat{y}, \mathcal{T}_x, \mathbf{H}_x)\}$ , block size  $B$ , generation length  $L_g$ , weights  $w_{\text{cons}}, w_{\text{distill}}, w_{\text{dlm}}$ , student DLM  $q_\phi(\cdot \mid x)$  with *block-wise causal attention*, total steps  $N=L_g$
- 2: **Output:** updated student parameters  $\phi$
- 3: **repeat**
- 4:   Sample  $(x, \hat{y}, \mathcal{T}_x, \mathbf{H}_x) \sim \mathcal{D}$
- 5:   Sample  $t_{\text{start}}$ ; set  $t_{\text{end}} \leftarrow \min(N, \lceil \frac{t_{\text{start}}}{B} \rceil B)$
- 6:   Retrieve states at  $t_{\text{start}}$  and  $t_{\text{end}}$  from  $\mathcal{T}_x$
- 7:   Compute  $\mathcal{L}_{\text{Distillation}}$  (Eq. (4)) using  $\mathbf{H}_x$
- 8:   Compute  $\mathcal{L}_{\text{Consistency}}$  (Eq. (5))
- 9:   Compute  $\mathcal{L}_{\text{DLM}}$  (Eq. (6)) using ground-truth text  $\hat{y}$
- 10:    $\mathcal{L} \leftarrow w_{\text{distill}} \mathcal{L}_{\text{Distillation}} + w_{\text{cons}} \mathcal{L}_{\text{Consistency}} + w_{\text{dlm}} \mathcal{L}_{\text{DLM}}$
- 11:   Update  $\phi$  with  $\mathcal{L}$
- 12: **until** max epochs

we minimize the following objective:

$$\mathcal{L}_{\text{Consistency}} = \mathbb{E}_{(x, \mathcal{T}_x) \sim \mathcal{D}} \mathbb{E}_{y \sim \mathcal{T}_x} \left[ \frac{1}{|\mathcal{S}_y|} \sum_{i \in \mathcal{S}_y} D_{\text{KL}}(q_{\phi^-}(\cdot \mid y^*, x)_i \parallel q_\phi(\cdot \mid y, x)_i) \right]. \quad (5)$$

Here,  $q_{\phi^-}$  denotes a stop-gradient target (detached from backpropagation) for stable training (Song et al., 2023), and  $D_{\text{KL}}$  is the forward KL divergence between two distributions. Intuitively, Eq. (5) aligns the student at a *less-informed* state with itself at a *more-informed* state, but only over  $\mathcal{S}_y$  where predictions are well-defined. Since DLMs are trained to predict only [MASK] tokens, restricting the loss to still-masked indices avoids ill-defined supervision and helps the model jump several steps in a stable, consistent manner.

**DLM loss** We include an auxiliary loss, identical to the masked denoising objective used in standard DLM pre-training (Nie et al., 2025b; Ye et al., 2025), to preserve the model’s mask prediction capability. For a prompt  $x$  and its ground-truth response  $\hat{y}$ , we randomly sample a masking ratio  $t \sim \mathcal{U}[0, 1]$  and independently mask each token with a probability  $t$  to obtain the masked sequence  $\hat{y}_t$ . The resulting objective is

$$\mathcal{L}_{\text{DLM}} = -\mathbb{E}_{(x, \hat{y}) \sim \mathcal{D}} \mathbb{E}_t \left[ \frac{1}{t} \sum_{i=1}^{L_g} \mathbf{1}[\hat{y}_{t,i} = [\text{MASK}]] \log q_\phi(\hat{y}_i \mid \hat{y}_t, x) \right]. \quad (6)$$

Here,  $\mathbf{1}[\cdot]$  denotes the indicator function.

Consequently, the total training objective is

$$\mathcal{L}(\phi) = w_{\text{distill}} \mathcal{L}_{\text{Distillation}} + w_{\text{cons}} \mathcal{L}_{\text{Consistency}} + w_{\text{dlm}} \mathcal{L}_{\text{DLM}}. \quad (7)$$

### 4.3 Inference

At inference time, the student decodes block-wise under a block-causal mask (Figure 2), reusing the KV cache for the prompt and all previously finalized blocks. Within each block, we apply *confidence-thresholded* parallel finalization: at each step, among the masked positions of the current block, we reveal every token whose confidence exceeds a threshold  $\tau_{\text{conf}}$ , following Fast-dLLM (Wu et al., 2025b). Larger  $\tau_{\text{conf}}$  yields more conservative decoding (typically higher quality but slower convergence), whereas smaller  $\tau_{\text{conf}}$  is more aggressive (faster convergence) at the cost of potential accuracy loss. We also adopt early stopping: decoding terminates once an `<endoftext>` token is produced within the current block, analogous to AR decoding. We intentionally avoid additional heuristics such as inter-block parallelism (Wang et al., 2025), which introduce extra hyperparameters whose optimal values are task- and domain-dependent.

## 5 EXPERIMENTS

### 5.1 Experimental Setup

This subsection summarizes datasets, CDLM training, evaluation protocol, baselines, hardware, and metrics.

**Target Models and Datasets** We evaluate two representative open-source DLMS: Dream-7B-Instruct (Ye et al., 2025) and LLaDA-8B-Instruct (Nie et al., 2025b). Our prompts are derived from Bespoke-Stratos-17k (Labs, 2025). Specifically, we use two publicly available datasets from the Hugging Face Hub (Lansehen, 2025a;b), retaining items whose prompt length is  $\leq 512$  tokens. For LLaDA, we further augment its corpus with 7.5k additional math-style prompts sourced from the DParallel dataset (Chen et al., 2025). For each prompt, we generate teacher trajectories at temperatures  $\{0.0, 0.5\}$  (greedy / non-greedy), yielding 15k generations for Dream and 30k for LLaDA. Generation uses the bidirectional, block-wise teacher with generation length  $L_g=256$ , block size  $B=32$ , and total steps  $N=256$ . Additional details are provided in Appendix A.1.

**Training Details** We fine-tune all models with LoRA (Hu et al., 2022) applied to the attention and MLP modules. Models are optimized with AdamW using a constant schedule with warmup. During CDLM training, we use a block-wise causal mask with block size 32 (see Figure 2). Prompts are left-padded to 512 tokens and the generation length is 256, yielding a fixed sequence length of 768. We set loss weights

to  $(w_{\text{distill}}, w_{\text{cons}}, w_{\text{dlm}}) = (1.0, 0.5, 0.01)$  for Dream and  $(1.0, 0.5, 0.1)$  for LLaDA. Each model is trained for 16 epochs with an effective batch size of 64, and we select the best epoch by validation performance, reporting results from the corresponding checkpoint. End-to-end training takes approximately **8 hours** for CDLM-Dream and **16 hours** for CDLM-LLaDA on  $4 \times$  NVIDIA A100 (80GB) GPUs. Additional details are in Appendix A.2.

**Benchmarks.** Following established conventions (Wang et al., 2025; Wu et al., 2025b), we evaluate mathematical reasoning and code generation on GSM8K, GSM8K-CoT (Cobbe et al., 2021), MATH (Hendrycks et al., 2021), HumanEval (Chen et al., 2021a), and MBPP (Austin et al., 2021b). We use the `lm_eval` framework (Gao et al., 2024a) and the *Instruct* task variants for the coding benchmarks. We report exact match scores on GSM8K, math-verify scores on MATH, and pass@1 results on HumanEval, HumanEval-Instruct, and MBPP-Instruct after standard post-processing. Coding tasks are evaluated zero-shot, and few-shot settings for math follow the original Dream and LLaDA papers. All efficiency measurements are taken on  $4 \times$  NVIDIA A100 (80 GB) GPUs with batch size 1 under data parallelism. Latency, total steps, and generation length are reported as per-sample averages over the evaluation set.

**Baselines.** As references, we evaluate the original DLMS under their official inference settings. For LLaDA, we enable block-wise decoding. Dream does not support block-wise decoding, so we extend the baseline accordingly. Because our work targets two orthogonal axes of inference acceleration of (1) KV caching and (2) step reduction, we include three inference-time baselines that isolate or combine these factors: (i) dLLM-Cache (Liu et al., 2025), which focuses on (1) via adaptive feature caching; (ii) Fast-dLLM (Parallel) (Wu et al., 2025b), which targets (2) via confidence thresholding; and (iii) Fast-dLLM (Parallel + Dual Cache) (Wu et al., 2025b), which combines (1) + (2) via approximate dual-cache KV caching. We omit D2F (Wang et al., 2025) here because it is trained for  $L_g=512$  and reports on Dream-7B-Base rather than Dream-7B-Instruct. For autoregressive comparisons, we evaluate Qwen2.5-7B-Instruct (Yang et al., 2024) alongside Dream and Llama-3.1-8B-Instruct (Dubey et al., 2024) alongside LLaDA. For fair comparison, we use a fixed generation length of  $L_g=256$ , greedy decoding (temperature 0.0), a block size of  $B=32$  for block-wise decoding, and a token-confidence threshold of  $\tau_{\text{conf}}=0.9$ . Further details are in Appendix A.3.

### 5.2 Main Results

We compare CDLM against vanilla DLMS, accelerated DLM variants, and autoregressive baselines, and summarize the quantitative results.

Table 1. Evaluation results for **Dream-7B-Instruct**. Arrows in headers indicate whether higher ( $\uparrow$ ) or lower ( $\downarrow$ ) is better. *Notes:* Par. = parallel decoding; D.C. = dual-cache KV.

| Benchmark                             | Method                | TPS $\uparrow$                | Latency (s) $\downarrow$     | Total Steps $\downarrow$     | Gen. Length | Score $\uparrow$ |
|---------------------------------------|-----------------------|-------------------------------|------------------------------|------------------------------|-------------|------------------|
| <b>GSM8K-CoT</b><br>(8-shot)          | Dream-7B-Instruct     | 4.1 ( $\times 1.0$ )          | 23.5 ( $\times 1.0$ )        | 256.0 ( $\times 1.0$ )       | 95.1        | 79.1             |
|                                       | dLLM-Cache            | 6.9 ( $\times 1.7$ )          | 12.6 ( $\times 1.9$ )        | 256.0 ( $\times 1.0$ )       | 87.5        | 75.2             |
|                                       | Fast-dLLM (Par.)      | 19.2 ( $\times 4.7$ )         | 5.0 ( $\times 4.7$ )         | 53.7 ( $\times 4.8$ )        | 96.0        | <b>79.9</b>      |
|                                       | Fast-dLLM (Par.+D.C.) | 36.6 ( $\times 8.9$ )         | 2.5 ( $\times 9.4$ )         | 60.8 ( $\times 4.2$ )        | 90.3        | 77.3             |
|                                       | CDLM-Dream (ours)     | <b>51.7</b> ( $\times 12.6$ ) | <b>2.1</b> ( $\times 11.2$ ) | <b>44.1</b> ( $\times 5.8$ ) | 107.4       | 78.8             |
| <b>HumanEval-Instruct</b><br>(0-shot) | Dream-7B-Instruct     | 15.4 ( $\times 1.0$ )         | 13.4 ( $\times 1.0$ )        | 256.0 ( $\times 1.0$ )       | 206.7       | 48.2             |
|                                       | dLLM-Cache            | 9.4 ( $\times 0.6$ )          | 12.0 ( $\times 1.1$ )        | 256.0 ( $\times 1.0$ )       | 113.6       | 43.9             |
|                                       | Fast-dLLM (Par.)      | 66.4 ( $\times 4.3$ )         | 3.2 ( $\times 4.2$ )         | 61.6 ( $\times 4.2$ )        | 210.2       | 45.7             |
|                                       | Fast-dLLM (Par.+D.C.) | <b>79.9</b> ( $\times 5.2$ )  | 2.5 ( $\times 5.4$ )         | 71.6 ( $\times 3.6$ )        | 200.9       | 46.3             |
|                                       | CDLM-Dream (ours)     | 43.3 ( $\times 2.8$ )         | <b>2.2</b> ( $\times 6.1$ )  | <b>49.6</b> ( $\times 5.2$ ) | 96.9        | <b>50.0</b>      |
| <b>MATH</b><br>(4-shot)               | Dream-7B-Instruct     | 8.3 ( $\times 1.0$ )          | 21.9 ( $\times 1.0$ )        | 256.0 ( $\times 1.0$ )       | 182.2       | <b>38.0</b>      |
|                                       | dLLM-Cache            | 11.3 ( $\times 1.4$ )         | 13.0 ( $\times 1.7$ )        | 256.0 ( $\times 1.0$ )       | 146.9       | 35.8             |
|                                       | Fast-dLLM (Par.)      | 23.9 ( $\times 2.9$ )         | 7.6 ( $\times 2.9$ )         | 87.1 ( $\times 2.9$ )        | 181.0       | 37.8             |
|                                       | Fast-dLLM (Par.+D.C.) | 48.8 ( $\times 5.9$ )         | 3.7 ( $\times 5.9$ )         | 98.2 ( $\times 2.6$ )        | 179.8       | 37.4             |
|                                       | CDLM-Dream (ours)     | <b>53.8</b> ( $\times 6.5$ )  | <b>2.9</b> ( $\times 7.6$ )  | <b>63.2</b> ( $\times 4.1$ ) | 158.4       | 32.4             |
| <b>MBPP-Instruct</b><br>(0-shot)      | Dream-7B-Instruct     | 2.3 ( $\times 1.0$ )          | 21.7 ( $\times 1.0$ )        | 256.0 ( $\times 1.0$ )       | 49.5        | 51.8             |
|                                       | dLLM-Cache            | 5.1 ( $\times 2.2$ )          | 11.3 ( $\times 1.9$ )        | 256.0 ( $\times 1.0$ )       | 57.3        | <b>56.0</b>      |
|                                       | Fast-dLLM (Par.)      | 15.5 ( $\times 6.7$ )         | 3.1 ( $\times 7.0$ )         | 35.3 ( $\times 7.3$ )        | 47.3        | 55.6             |
|                                       | Fast-dLLM (Par.+D.C.) | 25.4 ( $\times 11.0$ )        | 1.9 ( $\times 11.4$ )        | 43.6 ( $\times 5.9$ )        | 47.1        | 53.4             |
|                                       | CDLM-Dream (ours)     | <b>48.1</b> ( $\times 20.9$ ) | <b>1.5</b> ( $\times 14.5$ ) | <b>33.2</b> ( $\times 7.7$ ) | 74.3        | 53.0             |

### 5.2.1 Results on CDLM-Dream

Table 1 summarizes throughput, latency, step counts, generation length, and accuracy for Dream-7B-Instruct and its acceleration baselines.

**Steps and scores.** Our objective is to reduce the number of sampling steps so that the model reaches a coherent answer faster. As shown in Table 1, CDLM-Dream achieves the largest step reductions across benchmarks, cutting steps by roughly  $4.1\times$ – $7.7\times$  without significant accuracy degradation. The naive Dream baseline is typically run with 256 refinement steps to generate 256 tokens; simply reducing this step count markedly degrades quality (see the ablation in Section 5.3.2). Despite aggressive step reduction, CDLM-Dream matches or improves accuracy: it rises from 51.8→53.0 on MBPP-Instruct and from 48.2→50.0 on HumanEval-Instruct, with only a negligible drop on GSM8K-CoT (79.1→78.8). Note that dLLM-Cache keeps the step budget fixed at 256 and accelerates via KV caching rather than step reduction.

We attribute the drop on MATH to two factors. First, the small training mixture ( $\sim 7.5k$  prompts) limits exposure to the advanced problem-solving skills required by MATH. Since the mixture is drawn from filtered subsets of Bespoke-Stratos-17k that largely consist of problems Qwen2.5 can already solve, the effective difficulty range is likely narrower than that of MATH. Second, CDLM is a fine-tuning-based method trained with teacher trajectories capped at 256 generation tokens. While sufficient for other benchmarks, this shorter thinking budget may be inadequate for complex

multi-step reasoning. A natural next step would be to train with a 512-token budget, as D2F (Wang et al., 2025) does.

**Latency.** Our method also yields the largest latency reductions on every benchmark. Latency improves by up to  $11.2\times$  on GSM8K-CoT and  $14.5\times$  on MBPP-Instruct. These gains come from combining *step reduction* with *block-wise caching*. Comparing Dream-7B-Instruct with dLLM-Cache, and Fast-dLLM (Parallel) with Fast-dLLM (Parallel+Dual Cache), shows that approximate KV caching substantially lowers inference time, even when step counts are similar or higher, by eliminating recomputation. For example, on GSM8K-CoT the Parallel+Dual Cache variant halves latency (5.0 s→2.5 s) despite more refinement steps (53.7→60.8). CDLM-Dream goes further by training with a block-wise causal attention mask (Figure 2), which makes KV caching natural at inference time. This causal structure also enables early termination at block boundaries when `<endoftext>` appears, analogous to AR early stopping, so the model stops earlier and avoids redundant tokens.

**Throughput (TPS).** CDLM-Dream achieves the highest TPS on three out of four tasks, outperforming all baselines. On MBPP-Instruct, it jumps from 2.3 to 48.1 tokens/s (a  $20.9\times$  increase over the naive model). The one exception is HumanEval-Instruct, where our TPS is lower than Fast-dLLM baselines because our effective generation length is much shorter (about 97 tokens vs.  $\sim 200$  for the baselines). This can depress our measured TPS and inflate baseline TPS. Crucially, despite shorter generations, our pass@1 is higher, indicating that CDLM-Dream emits fewer redundant tokens

Table 2. Evaluation results for **LLaDA-8B-Instruct**. Arrows in headers indicate whether higher ( $\uparrow$ ) or lower ( $\downarrow$ ) is better. We report HumanEval (not HumanEval-Instruct), as the latter lowers overall baseline scores. *Notes:* Par. = parallel decoding; D.C. = dual-cache KV.

| Benchmark                                   | Method                | TPS $\uparrow$               | Latency (s) $\downarrow$    | Total Steps $\downarrow$     | Gen. Length | Score $\uparrow$ |
|---------------------------------------------|-----------------------|------------------------------|-----------------------------|------------------------------|-------------|------------------|
| <b>GSM8K</b><br>(4-shot)                    | LLaDA-8B-Instruct     | 8.2 ( $\times 1.0$ )         | 28.3 ( $\times 1.0$ )       | 256.0 ( $\times 1.0$ )       | 232.1       | 77.1             |
|                                             | dLLM-Cache            | 18.7 ( $\times 2.3$ )        | 12.3 ( $\times 2.3$ )       | 256.0 ( $\times 1.0$ )       | 229.6       | 78.5             |
|                                             | Fast-dLLM (Par.)      | 26.7 ( $\times 3.3$ )        | 8.7 ( $\times 3.3$ )        | 77.5 ( $\times 3.3$ )        | 231.3       | <b>78.6</b>      |
|                                             | Fast-dLLM (Par.+D.C.) | <b>54.6</b> ( $\times 6.7$ ) | 4.2 ( $\times 6.7$ )        | 85.0 ( $\times 3.0$ )        | 230.4       | 76.5             |
|                                             | CDLM-LLaDA (ours)     | 54.3 ( $\times 6.6$ )        | <b>3.3</b> ( $\times 8.6$ ) | <b>57.7</b> ( $\times 4.4$ ) | 177.3       | 73.9             |
| <b>HumanEval</b><br>(0-shot)                | LLaDA-8B-Instruct     | 7.4 ( $\times 1.0$ )         | 11.3 ( $\times 1.0$ )       | 256.0 ( $\times 1.0$ )       | 83.9        | 37.8             |
|                                             | dLLM-Cache            | 12.6 ( $\times 1.7$ )        | 10.8 ( $\times 1.0$ )       | 256.0 ( $\times 1.0$ )       | 135.9       | 39.0             |
|                                             | Fast-dLLM (Par.)      | 17.9 ( $\times 2.4$ )        | 4.6 ( $\times 2.5$ )        | 100.3 ( $\times 2.6$ )       | 83.1        | 36.6             |
|                                             | Fast-dLLM (Par.+D.C.) | 18.9 ( $\times 2.6$ )        | 4.2 ( $\times 2.7$ )        | 97.7 ( $\times 2.6$ )        | 80.2        | 36.0             |
|                                             | CDLM-LLaDA (ours)     | <b>50.9</b> ( $\times 6.9$ ) | <b>1.9</b> ( $\times 5.9$ ) | <b>32.3</b> ( $\times 7.9$ ) | 95.1        | <b>40.2</b>      |
| <b>MATH</b><br>(4-shot)                     | LLaDA-8B-Instruct     | 8.8 ( $\times 1.0$ )         | 25.7 ( $\times 1.0$ )       | 256.0 ( $\times 1.0$ )       | 226.4       | 24.1             |
|                                             | dLLM-Cache            | 22.7 ( $\times 2.6$ )        | 10.9 ( $\times 2.4$ )       | 256.0 ( $\times 1.0$ )       | 248.5       | 33.3             |
|                                             | Fast-dLLM (Par.)      | 25.1 ( $\times 2.9$ )        | 9.9 ( $\times 2.6$ )        | 96.9 ( $\times 2.6$ )        | 248.6       | <b>33.4</b>      |
|                                             | Fast-dLLM (Par.+D.C.) | 49.7 ( $\times 5.7$ )        | 5.0 ( $\times 5.1$ )        | 107.0 ( $\times 2.4$ )       | 248.2       | 32.5             |
|                                             | CDLM-LLaDA (ours)     | <b>50.2</b> ( $\times 5.7$ ) | <b>4.2</b> ( $\times 6.1$ ) | <b>75.3</b> ( $\times 3.4$ ) | 210.3       | 28.3             |
| <b>MBPP</b><br><b>-Instruct</b><br>(0-shot) | LLaDA-8B-Instruct     | 17.7 ( $\times 1.0$ )        | 11.4 ( $\times 1.0$ )       | 256.0 ( $\times 1.0$ )       | 201.0       | 40.8             |
|                                             | dLLM-Cache            | 18.5 ( $\times 1.0$ )        | 10.8 ( $\times 1.1$ )       | 256.0 ( $\times 1.0$ )       | 199.4       | 40.8             |
|                                             | Fast-dLLM (Par.)      | 21.2 ( $\times 1.2$ )        | 6.2 ( $\times 1.8$ )        | 59.1 ( $\times 4.3$ )        | 131.8       | <b>42.0</b>      |
|                                             | Fast-dLLM (Par.+D.C.) | 40.1 ( $\times 2.3$ )        | 3.4 ( $\times 3.4$ )        | 66.9 ( $\times 3.8$ )        | 134.7       | 35.0             |
|                                             | CDLM-LLaDA (ours)     | <b>60.6</b> ( $\times 3.4$ ) | <b>3.2</b> ( $\times 3.6$ ) | <b>58.0</b> ( $\times 4.4$ ) | 195.3       | 38.4             |

while maintaining or improving solution quality.

### 5.2.2 Results on CDLM-LLaDA

Table 2 summarizes throughput, latency, step counts, generation length, and accuracy for LLaDA-8B-Instruct and its acceleration baselines.

**Steps and scores.** As in CDLM-Dream, our goal is to reduce the number of refinement steps via consistency training. As shown in Table 2, CDLM-LLaDA delivers the largest step reductions across all four benchmarks, cutting steps by roughly  $3.4\times-7.9\times$ . Despite this aggressive reduction, CDLM-LLaDA improves HumanEval from  $37.8\rightarrow 40.2$  and MATH from  $24.1\rightarrow 28.3$ . MBPP-Instruct shows a slight drop ( $40.8\rightarrow 38.4$ ), yet still outperforms Fast-dLLM (Par.+D.C.) by 3.4 points at comparable throughput. GSM8K is the only benchmark with a clear degradation ( $77.1\rightarrow 73.9$ ), which we analyze below.

We hypothesize that the degradation mainly stems from limited data and the underlying sensitivity of LLaDA to fine-tuning. In our initial experiments, training CDLM-LLaDA on a small mixture of  $\sim 7.5k$  bespoke prompts already reduced GSM8K accuracy from  $77.1\rightarrow 72.1$ , while slightly improving MATH from  $24.1\rightarrow 25.4$ . Empirically, we find that LLaDA is sensitive to fine-tuning: even simple SFT tends to harm its math ability unless the training data are carefully curated and sufficiently large. To mitigate this, we augment the training set with an additional 7.5k math-focused prompts (Section 5.1) and retrain. This raises GSM8K from  $72.1\rightarrow 73.9$  and MATH from  $25.4\rightarrow 28.3$ , while preserving

coding benchmark scores. We expect that further scaling and balancing of the dataset would reduce the remaining GSM8K gap, and leave this for future work.

**Latency and Throughput (TPS).** CDLM-LLaDA attains the strongest latency reductions across all tasks; for example, on GSM8K latency falls from  $28.3\text{ s}\rightarrow 3.3\text{ s}$ . Throughput gains are likewise substantial, ranging from  $3.4\times$  to  $6.9\times$  relative to the naive LLaDA baseline. The role of KV caching is evident when step counts are similar: LLaDA vs. dLLM-Cache keeps 256 steps yet nearly halves latency on GSM8K ( $28.3\text{ s}\rightarrow 12.3\text{ s}$ ), and Fast-dLLM (Parallel) vs. (Parallel+Dual Cache) reduces GSM8K latency further ( $8.7\text{ s}\rightarrow 4.2\text{ s}$ ) even as steps increase ( $77.5\rightarrow 85.0$ ). CDLM-LLaDA goes beyond caching alone by also reducing refinement steps via *consistency* training while retaining block-wise causality for natural KV caching, yielding the best overall efficiency in both latency and TPS.

### 5.2.3 Comparison with Autoregressive Models

**Throughput.** In terms of throughput, CDLM improves naive DLMs by  $3\times-21\times$  and also surpasses equal-size autoregressive (AR) baselines. For Dream, we compare against Qwen2.5-7B-Instruct (Figure 3), where CDLM-Dream achieves  $1.21\times$  higher throughput on GSM8K-CoT and  $1.12\times$  on MBPP-Instruct. For LLaDA, we compare against Llama-3.1-8B-Instruct (Figure 4), where CDLM-LLaDA reaches  $1.27\times$  the throughput on GSM8K and  $4.17\times$  on HumanEval. Throughput here reflects both per-step cost and the number of refinement steps. A CDLM

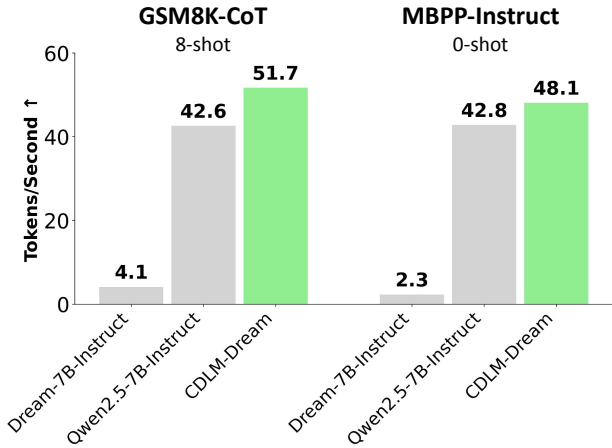


Figure 3. **Throughput vs. AR (Dream).** Tokens-per-second on GSM8K-CoT and MBPP-Instruct for Dream-7B-Instruct (naive), Qwen2.5-7B-Instruct (AR), and CDLM-Dream.

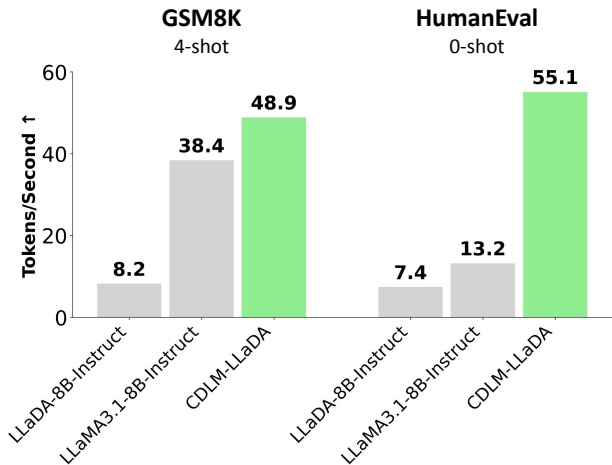


Figure 4. **Throughput vs. AR (LLaDA).** Tokens-per-second on GSM8K and HumanEval for LLaDA-8B-Instruct (naive), Llama3.1-8B-Instruct (AR), and CDLM-LLaDA.

refinement step is more expensive than an AR step due to matrix-matrix multiplications for decoding. However, CDLM can finalize multiple tokens per iteration, reducing total steps and increasing effective throughput. For example, from Table 1, CDLM-Dream produces on average  $107.4/44.1 \approx 2.4$  tokens per step on GSM8K-CoT and  $74.3/33.2 \approx 2.2$  tokens per step on MBPP-Instruct.

**Accuracy.** Although throughput is our focus, accuracy may be lower than that of AR models because CDLMs remain bounded by the strength of their DLM backbones. For CDLM-Dream versus its AR baseline, the accuracies are 78.8 vs. 73.8 on GSM8K-CoT and 53.0 vs. 81.7 on MBPP-Instruct (CDLM vs. AR). For CDLM-LLaDA versus its AR baseline, the respective accuracies are 73.9 vs. 80.3 on GSM8K and 40.2 vs. 60.4 on HumanEval (CDLM vs. AR). As stronger DLM backbones emerge, applying our

Table 3. **Ablation of loss weights.** We vary  $(w_{\text{distill}}, w_{\text{cons}}, w_{\text{dml}})$  and report *score* (top, black) and *steps to convergence* (bottom, blue) on GSM8K (4-shot) and HumanEval-Instruct (0-shot) for CDLM-Dream.

| $w_{\text{distill}}$ | $w_{\text{cons}}$ | $w_{\text{dml}}$ | GSM8K (4-shot) | HumanEval-Inst. (0-shot) |
|----------------------|-------------------|------------------|----------------|--------------------------|
| 1.0                  | ✗                 | 0.01             | 73.2<br>(46.7) | 42.7<br>(61.0)           |
| ✗                    | 1.0               | 0.01             | 6.9<br>(100.6) | 0.0<br>(124.3)           |
| 1.0                  | 1.0               | 0.01             | 74.1<br>(49.4) | 42.7<br>(49.4)           |
| 1.0                  | 1.0               | ✗                | 73.3<br>(46.2) | 48.2<br>(51.5)           |
| 1.0                  | 0.1               | 0.01             | 75.1<br>(48.0) | 45.7<br>(59.9)           |
| 1.0                  | 0.1               | ✗                | 73.7<br>(48.1) | 50.6<br>(69.0)           |

consistency-based fine-tuning should yield further throughput gains with improved quality.

### 5.3 Ablation Studies

We analyze how training and inference choices affect efficiency and accuracy.

#### 5.3.1 Loss-Weight Composition

Table 3 varies the loss weights  $(w_{\text{distill}}, w_{\text{cons}}, w_{\text{dml}})$  to study the trade-off between convergence speed and final accuracy. We train the Dream model for four epochs with a constant learning rate  $2e-5$ , then evaluate on GSM8K (4-shot) and HumanEval-Instruct (0-shot).

**Distillation vs. consistency in isolation.** With a small auxiliary DLM loss ( $w_{\text{dml}}=0.01$ ), the *distillation-only* setting (row 1) acts as a strong anchor: it converges quickly (about 46.7 and 61.0 steps for a generation length of 256), with a slight degradation in score. In contrast, *consistency-only* (row 2) collapses: optimizing for self-agreement without teacher supervision causes failure.

**Coupling yields synergy.** When we couple *consistency* with *distillation* (rows 3 and 5), convergence becomes both faster and more stable. GSM8K improves from 73.2 to 74.1–75.1 with similar or fewer steps, and HumanEval is comparable to or higher (42.7→45.7) while requiring fewer iterations. Intuitively, the student learns the teacher’s multi-token finalization while enforcing temporal self-consistency, which accelerates and stabilizes refinement.

**Role of the auxiliary DLM loss.** Removing the ground-truth masked-denoising term (rows 4 and 6) raises HumanEval but lowers GSM8K, indicating a loss of math

Table 4. **Ablation of refinement steps.** We report GSM8K results after naively truncating baseline DLM step counts to approximately match the step budgets used by CDLM–Dream and CDLM–LLaDA.

| Method            | Latency (s) ↓ | Steps ↓ | Score ↑ |
|-------------------|---------------|---------|---------|
| Dream-7B-Instruct | 4.4           | 48      | 41.8    |
| CDLM–Dream (ours) | 2.1           | 44.1    | 78.8    |
| LLaDA-8B-Instruct | 6.0           | 56      | 60.3    |
| CDLM–LLaDA (ours) | 3.3           | 57.7    | 73.9    |

Table 5. **Ablation of the confidence threshold.** We sweep the token-level threshold  $\tau_{\text{conf}}$  for CDLM–Dream on GSM8K-CoT (8-shot) and HumanEval-Instruct (0-shot).

| Benchmark        | $\tau_{\text{conf}}$ | TPS ↑       | Latency (s) ↓ | Score ↑     |
|------------------|----------------------|-------------|---------------|-------------|
| <b>GSM8K</b>     | 0.95                 | 42.7        | 2.5           | <b>78.8</b> |
| <b>-CoT</b>      | 0.90                 | 51.7        | 2.1           | <b>78.8</b> |
| (8-shot)         | 0.85                 | <b>57.7</b> | <b>1.9</b>    | 78.4        |
| <b>HumanEval</b> | 0.95                 | 34.4        | 2.8           | <b>51.2</b> |
| <b>-Instruct</b> | 0.90                 | 43.3        | 2.2           | 50.0        |
| (0-shot)         | 0.85                 | <b>47.3</b> | <b>2.0</b>    | 48.2        |

reasoning ability. A small auxiliary weight helps preserve this ability, and we find that general coding performance can be recovered with longer training.

Based on these trends, we fix  $w_{\text{distill}}=1.0$  and empirically choose  $w_{\text{cons}}=0.5$  as a good balance between speed and quality. For the auxiliary DLM loss, we use  $w_{\text{dlm}}=0.01$  for Dream and  $w_{\text{dlm}}=0.1$  for LLaDA, since the DLM loss on LLaDA has a smaller absolute scale.

### 5.3.2 Effective Step Reduction

We evaluate a naive step-truncation baseline by forcing the teacher DLMs to use a similar number of refinement steps as our CDLMs (Table 4). Because decoding is block-wise, the step count must be a multiple of the block factor ( $L_g/B=8$ ). For Dream, we set the step budget to 48 and measure GSM8K-CoT (8-shot) as in Table 1; for LLaDA, we set it to 56 and measure GSM8K (4-shot) as in Table 2. Naively truncating the step budget, in other words, forcing a non-retrained DLM to finalize multiple tokens per iteration, leads to marked accuracy degradation. By contrast, CDLM maintains quality while operating with substantially fewer steps, underscoring that consistency training is necessary for stable multi-token refinement. Furthermore, with KV caching, our approach reduces latency by roughly half relative to the naive DLM at comparable iteration counts.

### 5.3.3 Token-Level Confidence Threshold

Table 5 sweeps the token-level confidence threshold  $\tau_{\text{conf}} \in \{0.85, 0.90, 0.95\}$  to characterize conservative-aggressive decoding behavior. Increasing  $\tau_{\text{conf}}$  makes finalization more

conservative, tokens are only accepted when the model is highly confident, so throughput (TPS) decreases and per-sample latency increases. Decreasing  $\tau_{\text{conf}}$  makes decoding more aggressive and has the opposite effect. This monotonic speed trend holds on both GSM8K-CoT and HumanEval-Instruct. Concretely, on GSM8K-CoT, TPS/latency moves from 42.7/2.5 s at  $\tau=0.95$  to 57.7/1.9 s at  $\tau=0.85$ ; on HumanEval-Instruct, from 34.4/2.8 s to 47.3/2.0 s.

Accuracy shows a similar monotonic trend in  $\tau_{\text{conf}}$ . On GSM8K-CoT, scores are essentially flat at 78.8 for  $\tau=0.95$  and 0.90, with a slight drop at  $\tau=0.85$  (78.4). Similarly, on HumanEval-Instruct, the best score appears at the most conservative setting (51.2 at  $\tau=0.95$ ), 3 points higher than the most aggressive setting ( $\tau=0.85$ ). These results suggest that raising  $\tau_{\text{conf}}$  trades speed for quality, but the gain is not linear. In practice, we find  $\tau_{\text{conf}}=0.90$  to be a robust default that balances speed and quality across tasks.

## 6 DISCUSSION

Here, we discuss some complementary and future avenues for our work, as well as its limitations.

**Inference-only accelerations.** Our method complements and can be combined with various inference-only (non-trainable) acceleration techniques. At inference time, we use only block-wise KV caching and confidence-based multi-token finalization, but more sophisticated mechanisms can be layered on top. For example, one can incorporate D2F’s inter-block parallelism to further reduce wall-clock latency (Wang et al., 2025).

**DLM as a drafter.** Speculative decoding employs a smaller draft model to propose token bursts that a larger verifier accepts or rejects in parallel (Leviathan et al., 2023). A naive diffusion language model (DLM) drafter yields limited benefit because standard DLMs require many refinement steps to produce coherent text. In contrast, a *consistency*-trained DLM (CDLM) can generate reasonable drafts in far fewer steps. Pairing a CDLM drafter with an autoregressive (AR) verifier (cf. (Christopher et al., 2025)) is promising: the CDLM proposes multi-token candidates quickly, and the AR model supplies strong final validation.

**Limitations.** Training currently relies on offline, static trajectories. Despite careful dataset selection, the student may overfit to the teacher’s prior because supervision does not adapt during learning. For LLaDA, we observe that augmenting the training set with additional math-style prompts improves math performance by 2–3 percentage points while preserving other abilities, suggesting that scale and domain coverage are critical factors. Scaling beyond our current 15k-prompt corpus and broadening it to more diverse domains

are straightforward directions for future work. Furthermore, CDLM’s performance is bounded by the teacher: a bidirectional DLM distilled into a block-causal student cannot exceed the teacher’s knowledge. Distilling from stronger DLM or AR teachers is a natural way to lift this ceiling. Additional discussion appears in Appendix B.

## 7 CONCLUSION

We presented **CDLM**, a training-based acceleration scheme that brings *consistency modeling* to DLMS. By enforcing within-block temporal consistency and fine-tuning a block-wise causal student, CDLM reduces refinement steps and enables natural KV caching. Across math and coding tasks, it yields faster inference, fewer steps, lower latency, and higher throughput, while maintaining competitive accuracy. Promising directions include scaling the distillation corpus, broadening domain coverage, and distilling from stronger teachers.

## ACKNOWLEDGEMENTS

We acknowledge gracious support from the FuriosaAI, Intel, Apple, NVIDIA, Macronix, and Mozilla team. Furthermore, we appreciate support from Google Cloud, the Google TRC team and Prof. David Patterson. Prof. Keutzer’s lab is sponsored by the Intel corporation, UC Berkeley oneAPI Center of Excellence, Intel VLAB team, as well as funding through BDD and BAIR. We also acknowledge support by the Director, Office of Science, Office of Advanced Scientific Computing Research, of the U.S. Department of Energy under Contract No. DE-AC02-05CH11231. DOE SciGPT grant. Minseo also gratefully acknowledges the SNUCSE GPU Service 3.0 program and Bacchus for providing A100 GPU resources that supported this research. Our conclusions do not necessarily reflect the position or the policy of our sponsors, and no official endorsement should be inferred.

## REFERENCES

- Agarwal, R., Vieillard, N., Zhou, Y., Stanczyk, P., Ramos, S., Geist, M., and Bachem, O. On-policy distillation of language models: Learning from self-generated mistakes. In *Proceedings of the 12th International Conference on Learning Representations (ICLR)*, 2024. URL <https://arxiv.org/abs/2306.13649>.
- Austin, J., Johnson, D. D., Ho, J., Tarlow, D., and van den Berg, R. Structured denoising diffusion models in discrete state-spaces. In *Advances in Neural Information Processing Systems*, volume 34. Curran Associates, Inc., 2021a. URL <https://proceedings.neurips.cc/paper/2021/hash/958c530554f78bcd8e97125b70e6973d-Abstract.html>.
- Austin, J., Odena, A., Nye, M., Bosma, M., Michalewski, H., Dohan, D., Jiang, E., Cai, C., Terry, M., Le, Q., and Sutton, C. Program synthesis with large language models. *arXiv preprint arXiv:2108.07732*, 2021b. URL <https://arxiv.org/abs/2108.07732>.
- Ben-Hamu, H., Gat, I., Severo, D., Nolte, N., and Karrer, B. Accelerated sampling from masked diffusion models via entropy bounded unmasking. *arXiv preprint arXiv:2505.24857*, 2025. URL <https://arxiv.org/abs/2505.24857>.
- Chen, M., Tworek, J., Jun, H., Yuan, Q., de Oliveira Pinto, H. P., Kaplan, J., Edwards, H., Burda, Y., Joseph, N., Brockman, G., Ray, A., Puri, R., Krueger, G., Petrov, M., Khlaaf, H., Sastry, G., Mishkin, P., Chan, B., Gray, S., Ryder, N., Pavlov, M., Power, A., Kaiser, L., Bavarian, M., Winter, C., Tillet, P., Such, F. P., Cummings, D., Plappert, M., Chantzis, F., Barnes, E., Herbert-Voss, A., Guss, W. H., Nichol, A., Paino, A., Tezak, N., Tang, J., Babuschkin, I., Balaji, S., Jain, S., Saunders, W., Hesse, C., Carr, A. N., Leike, J., Achiam, J., Misra, V., Morikawa, E., Radford, A., Knight, M., Brundage, M., Murati, M., Mayer, K., Welinder, P., McGrew, B., Amodei, D., McCandlish, S., Sutskever, I., and Zaremba, W. Evaluating large language models trained on code. *arXiv preprint arXiv:2107.03374*, 2021a. URL <https://arxiv.org/abs/2107.03374>.
- Chen, N., Zhang, Y., Zen, H., Weiss, R. J., Norouzi, M., and Chan, W. Wavegrad: Estimating gradients for waveform generation. In *International Conference on Learning Representations*, 2021b. URL <https://arxiv.org/abs/2009.00713>.
- Chen, Z., Fang, G., Ma, X., Yu, R., and Wang, X. dparallel: Learnable parallel decoding for dllms. *arXiv preprint arXiv:2509.26488*, 2025. URL <https://arxiv.org/abs/2509.26488>.
- Christopher, J. K., Bartoldson, B. R., Ben-Nun, T., Cardei, M., Kailkhura, B., and Fioretto, F. Speculative diffusion decoding: Accelerating language generation through diffusion. In *Proceedings of the 2025 Conference of the North American Chapter of the Association for Computational Linguistics: Human Language Technologies (Volume 1: Long Papers)*, pp. 12042–12059, Albuquerque, New Mexico, 2025. Association for Computational Linguistics. doi: 10.18653/v1/2025.naacl-long.601. URL <https://aclanthology.org/2025.naacl-long.601/>.
- Cobbe, K., Kosaraju, V., Bavarian, M., Chen, M., Jun, H., Kaiser, L., Plappert, M., Tworek, J., Hilton, J., Nakano, R., Hesse, C., and Schulman, J. Training verifiers to solve math word problems. In *Proceedings of the 2021 Conference on Empirical Methods in Natural Language Processing (EMNLP)*, 2021. URL <https://arxiv.org/abs/2110.14168>.
- Deschenaux, J. and Gulcehre, C. Beyond autoregression: Fast llms via self-distillation through time. In *The Thirteenth International Conference on Learning Representations (ICLR)*, 2025. URL <https://openreview.net/forum?id=uZ5K4HeNwd>.
- Dubey, A., Jauhri, A., Pandey, A., Kadian, A., Al-Dahle, A., Letman, A., Mathur, A., Schelten, A., Yang, A., Fan, A., et al. The llama 3 herd of models. *arXiv preprint arXiv:2407.21783*, 2024. URL <https://arxiv.org/abs/2407.21783>.
- Esser, P., Chiu, J., Atighehchian, P., Granskog, J., and Germanidis, A. Structure and content-guided video synthesis with diffusion models. In *Proceedings of the IEEE/CVF International Conference on Computer Vision (ICCV)*, 2023. URL [https://openaccess.thecvf.com/content/ICCV2023/html/Esser\\_Structure\\_and\\_Content-Guided\\_Video\\_Synthesis\\_with\\_Diffusion\\_Models\\_ICCV\\_2023\\_paper.html](https://openaccess.thecvf.com/content/ICCV2023/html/Esser_Structure_and_Content-Guided_Video_Synthesis_with_Diffusion_Models_ICCV_2023_paper.html).
- Fu, Y., Peng, H., Ou, L., Sabharwal, A., and Khot, T. Specializing smaller language models towards multi-step reasoning. In *Proceedings of the 2023 International Conference on Machine Learning (ICML)*, pp. 10421–10430. PMLR, 2023. URL <https://proceedings.mlr.press/v202/fu23d.html>.
- Gao, L., Tow, J., Abbasi, B., Biderman, S., Black, S., DiPofi, A., Foster, C., Golding, L., Hsu, J., Le Noac’h, A., Li, H., McDonnell, K., Muennighoff, N., Ociepa, C., Phang, J., Reynolds, L., Schoelkopf, H., Skowron, A., Sutawika, L., Tang, E., Thite, A., Wang, B., Wang, K., and Zou, A. The language model evaluation harness, 07 2024a. URL <https://zenodo.org/records/12608602>.

- Gao, Z., Guo, J., Tan, X., Zhu, Y., Zhang, F., Bian, J., and Xu, L. Empowering diffusion models on the embedding space for text generation. In *Proceedings of the 2024 Conference of the North American Chapter of the Association for Computational Linguistics (NAACL)*, 2024b.
- Gong, S., Li, M., Feng, J., Wu, Z., and Kong, L. Diffuseq: Sequence to sequence text generation with diffusion models. In *International Conference on Learning Representations*, 2023. URL <https://openreview.net/forum?id=D8DUDJQKZg>.
- Gong, S., Agarwal, S., Zhang, Y., Ye, J., Zheng, L., Li, M., An, C., Zhao, P., Bi, W., Peng, H., Han, J., and Kong, L. Scaling diffusion language models via adaptation from autoregressive models. In *Proceedings of the 2025 International Conference on Learning Representations (ICLR)*, 2025a. URL <https://arxiv.org/abs/2410.17891>.
- Gong, S., Zhang, R., Zheng, H., Gu, J., Jaitly, N., Kong, L., and Zhang, Y. Diffucoder: Understanding and improving masked diffusion models for code generation. *arXiv preprint arXiv:2506.20639*, June 2025b. doi: 10.48550/arXiv.2506.20639. URL <https://arxiv.org/abs/2506.20639>.
- Google DeepMind. Gemini Diffusion. <https://deepmind.google/models/gemini-diffusion/>, 2025.
- Gu, Y., Dong, L., Wei, F., and Huang, M. Minillm: Knowledge distillation of large language models. *arXiv preprint arXiv:2306.08543*, 2023. URL <https://arxiv.org/abs/2306.08543>.
- Hendrycks, D., Burns, C., Kadavath, S., Arora, A., Basart, S., Tang, E., Song, D., and Steinhardt, J. Measuring mathematical problem solving with the MATH dataset. In *NeurIPS 2021 Datasets and Benchmarks Track (Round 2)*, 2021. URL <https://datasets-benchmarks-proceedings.neurips.cc/paper/2021/file/be83ab3ecd0db773eb2dclb0a17836a1-Paper-round2.pdf>.
- Hinton, G., Vinyals, O., and Dean, J. Distilling the knowledge in a neural network. *arXiv preprint arXiv:1503.02531*, 2015. URL <https://arxiv.org/abs/1503.02531>.
- Ho, J., Jain, A., and Abbeel, P. Denoising diffusion probabilistic models. In *Advances in Neural Information Processing Systems*, 2020.
- Hu, E. J., Shen, Y., Wallis, P., Allen-Zhu, Z., Li, Y., Wang, S., Wang, L., and Chen, W. LoRA: Low-rank adaptation of large language models. In *The Tenth International Conference on Learning Representations*, 2022. URL <https://openreview.net/forum?id=nZeVKeeFYf9>.
- Hu, J. C., Cavicchioli, R., and Capotondi, A. Bidirectional awareness induction in autoregressive seq2seq models. *arXiv preprint arXiv:2408.13959*, 2024. URL <https://arxiv.org/abs/2408.13959>.
- Hu, Z., Meng, J., Akhauri, Y., Abdelfattah, M. S., Seo, J.-s., Zhang, Z., and Gupta, U. Accelerating diffusion language model inference via efficient kv caching and guided diffusion. *arXiv preprint arXiv:2505.21467*, 2025. URL <https://arxiv.org/abs/2505.21467>.
- Khanna, S., Kharbanda, S., Li, S., Varma, H., Wang, E., Birnbaum, S., Luo, Z., Miraoui, Y., Palrecha, A., Ermon, S., Grover, A., and Kuleshov, V. Mercury: Ultra-fast language models based on diffusion. *arXiv preprint arXiv:2506.17298*, 2025. URL <https://arxiv.org/abs/2506.17298>.
- Kim, M., Hooper, C., Tomar, A., Xu, C., Farajtabar, M., Mahoney, M. W., Keutzer, K., and Gholami, A. Beyond next-token prediction: A performance characterization of diffusion versus autoregressive language models. *arXiv preprint arXiv:2510.04146*, 2025. URL <https://arxiv.org/abs/2510.04146>.
- Kou, S., Hu, L., He, Z., Deng, Z., and Zhang, H. Cllms: Consistency large language models. In *Proceedings of the 41st International Conference on Machine Learning (ICML)*, pp. 25426–25440. PMLR, 2024. URL <https://arxiv.org/abs/2403.00835>.
- Labs, B. Bespoke-stratos: The unreasonable effectiveness of reasoning distillation. <https://www.bespokelabs.ai/blog/bespoke-stratos-the-unreasonable-effectiveness-of-reasoning-distillation>, 2025. Accessed: 2025-01-22.
- Lansecchen. Lansecchen/bs17k\_collection\_filtered\_easy\_maxlength600. [https://huggingface.co/datasets/Lansecchen/bs17k\\_collection\\_filtered\\_easy\\_maxlength600](https://huggingface.co/datasets/Lansecchen/bs17k_collection_filtered_easy_maxlength600), 2025a. Accessed: 2025-10-23.
- Lansecchen. Lansecchen/bs17k\_collection\_filtered\_hard\_maxlength600. [https://huggingface.co/datasets/Lansecchen/bs17k\\_collection\\_filtered\\_hard\\_maxlength600](https://huggingface.co/datasets/Lansecchen/bs17k_collection_filtered_hard_maxlength600), 2025b. Accessed: 2025-10-23.
- Leviathan, Y., Kalman, M., and Matias, Y. Fast inference from transformers via speculative decoding. In *Proceedings of the 40th International Conference on Machine Learning*, volume 202, pp. 19274–19286. PMLR,

2023. URL <https://proceedings.mlr.press/v202/leviathan23a.html>.
- Li, X. L., Thickstun, J., Gulrajani, I., Liang, P. S., and Hashimoto, T. B. Diffusion-LM improves controllable text generation. In *Advances in Neural Information Processing Systems*, volume 35, pp. 4328–4343, 2022.
- Liu, Z., Yang, Y., Zhang, Y., Chen, J., Zou, C., Wei, Q., Wang, S., and Zhang, L. dllm-cache: Accelerating diffusion large language models with adaptive caching. *arXiv preprint arXiv:2506.06295*, 2025. URL <https://arXiv.org/abs/2506.06295>.
- Ma, X., Yu, R., Fang, G., and Wang, X. dkv-cache: The cache for diffusion language models. *arXiv preprint arXiv:2505.15781*, 2025. URL <https://arxiv.org/abs/2505.15781>.
- Nie, S., Zhu, F., Du, C., Pang, T., Liu, Q., Zeng, G., Lin, M., and Li, C. Scaling up masked diffusion models on text. In *Proceedings of the 2025 International Conference on Learning Representations (ICLR)*, 2025a. URL <https://arXiv.org/abs/2410.18514>. Poster.
- Nie, S., Zhu, F., You, Z., Zhang, X., Ou, J., Hu, J., Zhou, J., Lin, Y., Wen, J.-R., and Li, C. Large language diffusion models. *arXiv preprint arXiv:2502.09992*, 2025b. URL <https://arxiv.org/abs/2502.09992>.
- OpenAI. GPT-4 technical report. *arXiv preprint arXiv:2303.08774*, 2023. URL <https://arxiv.org/abs/2303.08774>.
- Ramesh, A., Dhariwal, P., Nichol, A., Chu, C., and Chen, M. Hierarchical text-conditional image generation with CLIP latents. *arXiv preprint arXiv:2204.06125*, 2022. URL <https://arxiv.org/abs/2204.06125>.
- Santilli, A., Severino, S., Postolache, E., Maiorca, V., Mancusi, M., Marin, R., and Rodola, E. Accelerating transformer inference for translation via parallel decoding. In *Proceedings of the 61st Annual Meeting of the Association for Computational Linguistics (Volume 1: Long Papers)*, pp. 12336–12355, Toronto, Canada, July 2023. Association for Computational Linguistics. doi: 10.18653/v1/2023.acl-long.689. URL <https://aclanthology.org/2023.acl-long.689/>.
- Song, Y. and Dhariwal, P. Improved techniques for training consistency models. *arXiv preprint arXiv:2310.14189*, 2023. URL <https://arXiv.org/abs/2310.14189>.
- Song, Y., Dhariwal, P., Chen, M., and Sutskever, I. Consistency models. In Krause, A., Brunskill, E., Cho, K., Engelhardt, B., Sabato, S., and Scarlett, J. (eds.), *Proceedings of the 40th International Conference on Machine Learning (ICML)*, volume 202 of *Proceedings of Machine Learning Research*, pp. 32211–32252. PMLR, 2023. URL <https://proceedings.mlr.press/v202/song23a.html>.
- Song, Y., Zhang, Z., Luo, C., Gao, P., Xia, F., Luo, H., Li, Z., Yang, Y., Yu, H., Qu, X., Fu, Y., Su, J., Zhang, G., Huang, W., Wang, M., Yan, L., Jia, X., Liu, J., Ma, W.-Y., Zhang, Y.-Q., Wu, Y., and Zhou, H. Seed diffusion: A large-scale diffusion language model with high-speed inference. *arXiv preprint arXiv:2508.02193*, 2025. URL <https://arxiv.org/abs/2508.02193>.
- Wang, X., Xu, C., Jin, Y., Jin, J., Zhang, H., and Deng, Z. Diffusion llms can do faster-than-ar inference via discrete diffusion forcing. *arXiv preprint arXiv:2508.09192*, 2025. URL <https://arXiv.org/abs/2508.09192>.
- Wu, C., Zhang, H., Xue, S., Diao, S., Fu, Y., Liu, Z., Molchanov, P., Luo, P., Han, S., and Xie, E. Fast-dllm v2: Efficient block-diffusion llm. *arXiv preprint arXiv:2509.26328*, 2025a. URL <https://arxiv.org/abs/2509.26328>.
- Wu, C., Zhang, H., Xue, S., Liu, Z., Diao, S., Zhu, L., Luo, P., Han, S., and Xie, E. Fast-dllm: Training-free acceleration of diffusion llm by enabling kv cache and parallel decoding. *arXiv preprint arXiv:2505.22618*, 2025b. URL <https://arxiv.org/abs/2505.22618>.
- Xu, C., Wang, X., Hou, T., Li, Y., and Deng, Z. dinfer: An efficient inference framework for diffusion language models. *arXiv preprint arXiv:2510.08666*, 2025a. URL <https://arxiv.org/abs/2510.08666>.
- Xu, C., Wang, X., Liao, Z., Li, Y., Hou, T., and Deng, Z. Unicms: A unified consistency model for efficient multimodal generation and understanding. *arXiv preprint arXiv:2502.05415*, 2025b. URL <https://arxiv.org/abs/2502.05415>.
- Yang, A., Yang, B., Zhang, B., Hui, B., Zheng, B., Yu, B., Li, C., Liu, D., Huang, F., Wei, H., Lin, H., Yang, J., Tu, J., Zhang, J., Yang, J., Yang, J., Zhou, J., Lin, J., Dang, K., Lu, K., Bao, K., Yang, K., Yu, L., Li, M., Xue, M., Zhang, P., Zhu, Q., Men, R., Lin, R., Li, T., Tang, T., Xia, T., Ren, X., Ren, X., Fan, Y., Su, Y., Zhang, Y., Wan, Y., Liu, Y., Cui, Z., Zhang, Z., Qiu, Z., and Qwen Team. Qwen2.5 technical report. *arXiv preprint arXiv:2412.15115*, December 2024. doi: 10.48550/arXiv.2412.15115. URL <https://arxiv.org/abs/2412.15115>.
- Ye, J., Xie, Z., Zheng, L., Gao, J., Wu, Z., Jiang, X., Li, Z., and Kong, L. Dream 7b: Diffusion large language models. *arXiv preprint arXiv:2508.15487*, 2025. URL <https://arxiv.org/abs/2508.15487>.

Yin, T., Gharbi, M., Zhang, R., Shechtman, E., Durand, F., Freeman, W. T., and Park, T. One-step diffusion with distribution matching distillation. In *Proceedings of the IEEE/CVF Conference on Computer Vision and Pattern Recognition (CVPR)*, pp. 6613–6623. IEEE / CVF, 2024. URL <https://arXiv.org/abs/2311.18828>.

Yin, T., Zhang, Q., Zhang, R., Freeman, W. T., Durand, F., Shechtman, E., and Huang, X. From slow bidirectional to fast autoregressive video diffusion models. In *Proceedings of the IEEE/CVF Conference on Computer Vision and Pattern Recognition (CVPR)*, pp. 22963–22974. IEEE / CVF, 2025. URL <https://arXiv.org/abs/2412.07772>.

Zhang, S., Roller, S., Goyal, N., Artetxe, M., et al. OPT: Open pre-trained transformer language models. *arXiv preprint arXiv:2205.01068*, 2022. URL <https://arxiv.org/abs/2205.01068>.

## A ADDITIONAL EXPERIMENTAL DETAILS

### A.1 Dataset and Preprocessing

**Sources.** We use two datasets (Lansechen, 2025a;b), which are post-processed versions of Bespoke-Stratos 17k (Labs, 2025). We choose them because (i) D2F (Wang et al., 2025), a representative fine-tuning-based DLM acceleration method, uses the same source, and (ii) they are filtered to a maximum length of 600 tokens and predominantly contain math word-style reasoning problems. For both Dream and LLaDA, we treat Qwen2.5-7B’s responses as ground-truth answers.

Dream is trained only on this Bespoke-derived subset. To strengthen math performance for LLaDA, we further augment its corpus with an additional 7.5k math-style prompts sampled from the DParallel dataset (Chen et al., 2025), matching the number of Bespoke-derived prompts. The released DParallel corpus does not include Qwen2.5-7B outputs, so we generate reference answers with Qwen2.5-7B for these prompts, yielding an LLaDA training set whose size is approximately  $2\times$  that of Dream. After trying multiple datasets, we empirically observe that dataset selection is crucial; overly rigid formats (e.g., multiple-choice math) tend to hurt the model’s ability to generalize.

**Temperature augmentation.** In DLMs, temperature influences not only token choices but also the *order* in which tokens are revealed (Gong et al., 2025b). We therefore generate multiple trajectories per prompt at different temperatures. However, as shown in Figure 5,  $\tau=1.0$  often destabilizes the reasoning chain and can yield incorrect conclusions. Consequently, we restrict trajectory collection to  $\tau \in \{0.0, 0.5\}$ .

**Hidden-state buffer.** Beyond token trajectories, we store the teacher’s decisions in a compact hidden-state buffer. Whenever a token is finalized, we record the teacher’s last-layer hidden state at that position; over a generation of length  $L_g$ , this yields a buffer of shape  $d \times L_g$  per example (see Figure 6). Directly saving logits is impractical because their dimensionality is  $|V|$  (vocabulary size); using hidden states of dimension  $d$  instead gives roughly a  $30\times$  reduction in storage. The trajectory datasets fit on a single server: each shard is 25-30 GiB for 15k samples.

### A.2 Training

**Training Configurations.** Full configurations are listed in Tables 6 and 7. Training ran on  $4\times$  NVIDIA A100 (80 GB) or  $8\times$  NVIDIA RTX A6000 (48 GB) GPUs; each epoch took roughly 30 minutes for 15k trajectories. We used per-device batch sizes of 1–2 with gradient accumulation to keep the effective batch size fixed at 64.

Table 6. Training configuration for **CDLM–Dream-7B-Instruct**.

|                                                                        |                                                                     |
|------------------------------------------------------------------------|---------------------------------------------------------------------|
| Learning rate                                                          | $2 \times 10^{-5}$                                                  |
| Scheduler (warmup)                                                     | constant (5%)                                                       |
| Epochs (best)                                                          | 16 (best: 12)                                                       |
| Effective batch size                                                   | 64                                                                  |
| Optimizer                                                              | AdamW                                                               |
| LoRA rank / $\alpha$                                                   | 32 / 32                                                             |
| LoRA targets                                                           | q_proj, k_proj, v_proj,<br>o_proj, up_proj,<br>down_proj, gate_proj |
| Prompt / generation length                                             | 512 / 256                                                           |
| Loss weights ( $w_{\text{distill}}, w_{\text{cons}}, w_{\text{dlm}}$ ) | (1.0, 0.5, 0.01)                                                    |

Table 7. Training configuration for **CDLM–LLaDA-8B-Instruct**.

|                                                                        |                                                                  |
|------------------------------------------------------------------------|------------------------------------------------------------------|
| Learning rate                                                          | $1 \times 10^{-5}$                                               |
| Scheduler (warmup)                                                     | constant (5%)                                                    |
| Epochs (best)                                                          | 16 (best: 12)                                                    |
| Effective batch size                                                   | 64                                                               |
| Optimizer                                                              | AdamW                                                            |
| LoRA rank / $\alpha$                                                   | 64 / 64                                                          |
| LoRA targets                                                           | q_proj, k_proj, v_proj,<br>attn_out, up_proj,<br>ff_proj, ff_out |
| Prompt / generation length                                             | 512 / 256                                                        |
| Loss weights ( $w_{\text{distill}}, w_{\text{cons}}, w_{\text{dlm}}$ ) | (1.0, 0.5, 0.1)                                                  |

**Loss formulations.** Empirically, the *forward* KL divergence yielded more stable, better-calibrated training dynamics and more monotonic convergence than the *reverse* KL divergence for distribution matching. We also found that distillation in *logit space* outperformed embedding-space distillation using mean squared error (MSE).

### A.3 Evaluation

**Hardware and parallelism.** All measurements in Section 5 except Table 3 were taken on  $4\times$  NVIDIA A100-80 GiB GPUs using data parallelism with batch size 1 per GPU.

**Tooling and post-processing.** We use `lm_eval` (EleutherAI’s `lm-eval-harness`) for dataset loading, prompting, and scoring. We apply the harness’s default post-processors. Decoded text is truncated at any task-specific `stop_sequences` prior to scoring. For HumanEval and MBPP, we additionally employ Python post-processing scripts adapted from the `dParallel` repository (Chen et al., 2025) to handle code execution and `pass@1` computation.

**Timing and metrics.** We report *per-sample averages*. End-to-end latency is computed by summing the wall-clock time of the generation routine across all ranks and dividing by the total number of evaluated samples. *Total steps* denotes the average number of refinement steps actually

Prompt: Return your final response within `\boxed{}`. Evaluate the product  $(n-1) \cdot n \cdot (n+1) \cdot (n+2) \cdot (n+3)$ , when  $n=2$ .

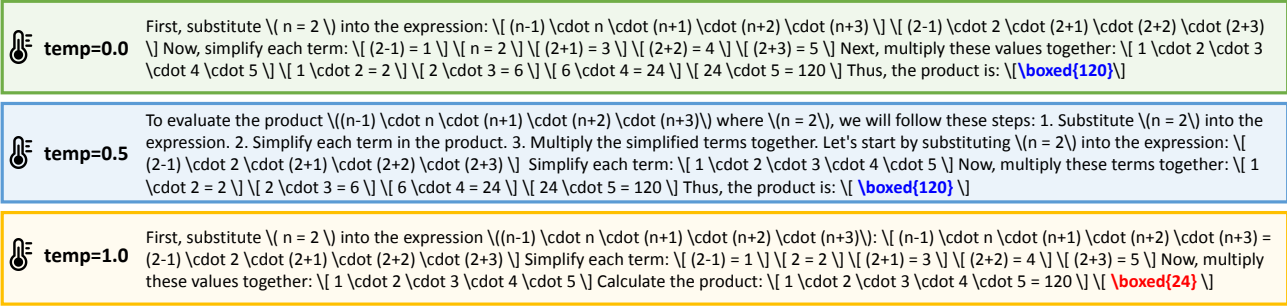


Figure 5. Teacher outputs vs. temperature. Final outputs from LLaDA-8B-Instruct at sampling temperatures  $\tau \in \{0.0, 0.5, 1.0\}$ . Answers are marked with `\boxed{}` (blue = correct; red = incorrect).

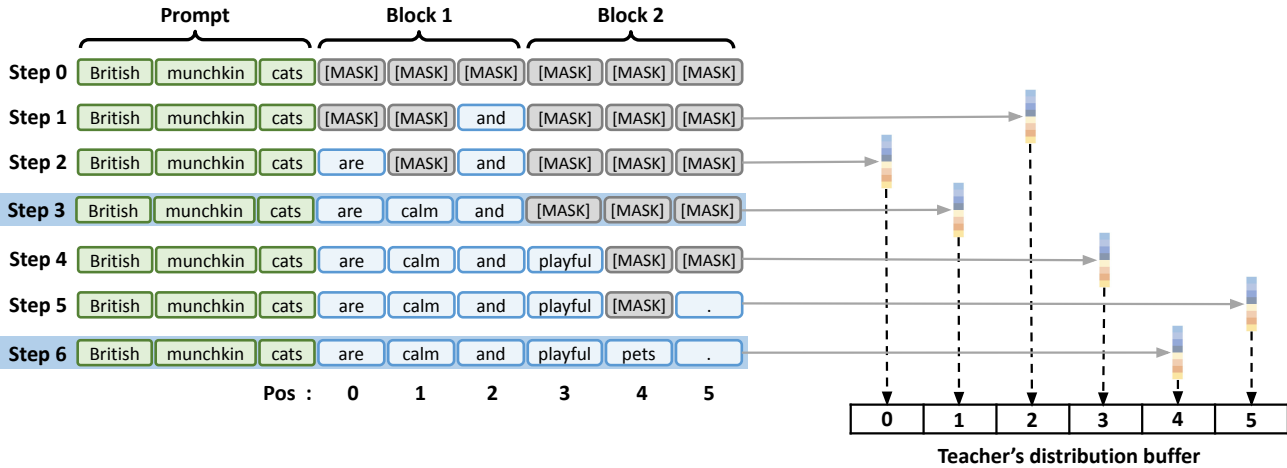


Figure 6. Teacher trajectory and hidden-state buffer. Left: Block-wise decoding trajectory. Right: As each token is finalized, the teacher's last hidden state at that position is written to a fixed-length buffer of size  $L_g$ ; arrows indicate write indices across steps (toy example with  $B=3, L_g=6$ ).

executed per sample (summed across ranks, then divided by the sample count). *Generation length* is the average number of valid tokens produced per sample, excluding `<endoftext>` and any content following a task-specific `stop_sequence`.

**Prompt formatting.** We follow each benchmark's standard few-shot protocol and, by default, apply the model's chat template. For HumanEval with LLaDA-8B-Instruct, however, enabling the chat template caused a sharp pass@1 decline (naive LLaDA: 37.8→7.9), so we evaluate HumanEval without the chat template. For math benchmarks, we do not use `--fewshot_as_multiturn`. Instead, all few-shot examples are merged into a single user prompt.

## B LIMITATIONS AND FUTURE DIRECTIONS

Our current training relies on offline, static trajectories. Although we carefully select datasets to limit domain bias, the student can still overfit to the teacher's priors because supervision does not adapt during training. A straightforward

direction is to broaden the data mixture and scale beyond our current ~15k samples, covering more domains.

A complementary path is to move from offline supervision to on-the-fly generation. If the student generates trajectories during training and the teacher verifies or refines them online, we can incorporate on-policy learning to reduce the training-inference discrepancy. In practice, this is currently constrained by DLM sampling speed: slow generation limits the feasibility of closed-loop training without prior trajectory materialization. Improving DLM inference throughput is therefore a prerequisite for large-scale online training.

CDLM's performance is ultimately bounded by the teacher: a bidirectional DLM distilled into a block-causal student cannot exceed the teacher's knowledge. To lift this ceiling, distillation from **stronger autoregressive (AR) teachers** is a natural next step. In this work we intentionally used high-quality, third-party-curated Qwen2.5-7B generations (Lansechen, 2025a;b) as ground-truth text, hoping to inject AR knowledge into the student. A more direct, and likely more effective, approach is to distill from an AR

teacher: AR models are already scaled up, typically stronger, and much faster at generation than naive DLMs, making large-scale dataset construction easier. Moreover, distillation is well suited to transferring knowledge from a larger, more powerful model to smaller students (here, Dream-7B and LLaDA-8B).